

# Amorphous Diblock Copolymers with a High Organometallic Block Volume Fraction: Synthesis, Characterization and Self-Assembly of Polystyrene-*block*-Poly(ferrocenylethylmethylsilane) in the Bulk State

Jean-Charles Eloi,<sup>†</sup> David A. Rider,<sup>‡</sup> Jia-Yu Wang,<sup>§</sup> Thomas P. Russell,<sup>§</sup> and Ian Manners<sup>\*,†</sup>

School of Chemistry, University of Bristol, Bristol, BS8 1TS United Kingdom, Department of Chemistry, University of Toronto, Toronto, ON M5S 3H6 Canada, and Department of Polymer Science and Engineering, University of Massachusetts, Amherst, Massachusetts 01003

Received June 4, 2008

Revised Manuscript Received September 9, 2008

**ABSTRACT:** The preparation of polystyrene-*b*-poly(ferrocenylethylmethylsilane) diblock copolymers (PS-*b*-PFEMS) with a high volume fraction of the organometallic block ( $\phi_{\text{PFEMS}} = 0.69\text{--}0.87$ ) has been achieved via the sequential living anionic polymerization of styrene and ethylmethylsila[1]ferrocenophane. High molecular weights ( $M_n = 50000$  to  $250000$  g/mol) and narrow molecular weight distributions ( $\text{PDI} = 1.05\text{--}1.17$ ) were achieved. As both of the blocks are amorphous, the resulting diblock copolymers undergo predictable self-assembly in the bulk and well-ordered microdomains are reported. The data described complement previous results on analogous block copolymers with a low PFEMS volume fraction and a morphology diagram for PS-*b*-PFEMS is described.

## Introduction

The self-assembly of block copolymers in the bulk and solution gives a wide range of well-studied morphologies.<sup>1</sup> This microphase-separation allows the fabrication of well-ordered nanostructured arrays of polymeric materials.<sup>2–4</sup> The introduction of a metal-containing block provides functional materials with new properties that complement those available with organic blocks.<sup>5–7</sup> For example, polyferrocenylsilane (PFS) block copolymers<sup>8–27</sup> possess a series of useful characteristics, such as redox-activity,<sup>10,11</sup> semiconductivity,<sup>12</sup> plasma etch resistance,<sup>13,14</sup> a high refractive index,<sup>15</sup> and also the ability to act as a precursor to magnetic<sup>16</sup> and catalytically active<sup>17–19</sup> metal nanoparticles. We have previously studied the amorphous polystyrene-*block*-poly(ferrocenylethylmethylsilane), PS-*b*-PFEMS, diblock copolymers with a low volume fraction of the organometallic block,<sup>28,29</sup> and the appropriate half of the morphology diagram has been reported. However, until now, the synthesis of PFS segments with sufficient lengths for the formation of block copolymers with a high organometallic volume fraction has been a challenge. In this paper, we report the synthesis of diblock copolymers containing a majority fraction of the unsymmetrically<sup>28</sup> substituted, amorphous polyferrocenylsilane PFEMS and the corresponding solid state morphological characterization.

## Experimental Section

**Equipment and Materials.** All polymerizations, storage of dry solvents and reagents, and handling of pyrophoric products and air and moisture sensitive monomers were performed in an MBraun MB 150B-G inert atmosphere glovebox purged with purified argon. All reagent distillations and monomer syntheses were carried out using Schlenk line techniques in a ventilated fume hood. <sup>1</sup>H NMR were performed on Jeol GX270 and Jeol GX400 at 270 and 400 MHz, respectively. Gel permeation chromatographies were carried out both on aliquots and diblocks using a Viscotek VE 2001 Triple-Detector Gel Permeation Chromatograph, equipped with an automatic sampler, a pump, an injector, an inline degasser, and a column oven (30 °C). The elution columns consist of styrene/divinyl benzene gels with pore sizes of 500 and 100000 Å. Detection was conducted by mean of a VE 3580 refractometer, a four-capillary differential viscometer, and a 90° and low angle (7°) laser light ( $\lambda_0 = 670$  nm) scattering detector, VE 3210 and VE 270. THF (Fisher) was used as the eluent, with a flow rate of 1.0 mL/min. Samples were dissolved in the eluent (2 mg/mL) and filtered with a Ministart SRP 15 filter (polytetrafluoroethylene membrane of 0.45  $\mu\text{m}$  pore size) before analysis. The calibration was conducted using a polystyrene solution from Viscotek. Block copolymer samples were dried in a Shel Laboratory vacuum oven, equipped with a nitrogen purge line. Bulk samples were microtomed at room temperature using a RMC MTXL ultramicrotome and a diamond knife. Copper grids from Agar Scientific, mesh 400, were coated with a carbon film. Carbon coating was done using an Agar TEM Turbo Carbon Coater, where carbon was sputtered onto mica sheets before deposition on the grids via flotation. Transmission electron microscopy (TEM) was performed on both Jeol 1200EX TEM Mk1 and Mk2. Both operate with a tungsten filament operated at 120 kV. They are fitted with a MegaViewII digital camera, using Soft Imaging Systems GmbH analySIS 3.0 image analysis software. Differential scanning calorimetry analyses were performed on a Q100 from TA instruments coupled to a refrigerated cooling system (RCS90). The samples, placed in nonhermetic aluminum pans, were tared using a XT220A Precisa microbalance. Small angle X-ray (SAXS) patterns were obtained from an Osmic MaxFlux X-ray source with a wavelength of 1.54 Å (Molecular Metrology, Inc.) and a camera consisting of a three-pinhole collimation system. The detector was a two-dimensional, multiwire proportional detector (Molecular Metrology, Inc.) and the distance sample-to-detector was 150 cm (calibrated using silver behenate).

Ferrocene was used in a ground form generated from pellets received from Octel Germany. Tetramethylethylenediamine was distilled from CaH<sub>2</sub>. Butyllithium and *sec*-butyllithium were used as received from Aldrich. Hexanes and diethylether were purified using Anhydrous Engineering double alumina and alumina/copper catalyst drying columns. Methanol, used for quenching the polymers, was deoxygenated by dinitrogen bubbling and then degassed. Tetrahydrofuran was distilled from Na/benzophenone under reduced pressure prior each experiment. Cyclohexane was dried over CaH<sub>2</sub> and refluxed for 3 h in a greaseless Perkins triangle and then distilled prior to use. Styrene was dried over CaH<sub>2</sub>, distilled under reduced atmosphere and stored over CaH<sub>2</sub>. When needed, it was distilled prior to each synthesis.

**Synthesis of Dilithioferrocene•Tetramethylethylenediamine.** Following a modification of the procedure<sup>30</sup> from a previous publication,<sup>28</sup> a ferrocene slurry (50 g, 0.27 mol) was made from hexanes (750 mL) under nitrogen to which was added dried tetramethylethylenediamine (50 mL, 0.33 mol) and chilled *n*-butyllithium (400 mL, 1.6 M) dropwise. The reaction was allowed to stir for three days. After successive washings with hexanes, the solid was dried overnight under vacuum and collected in an argon purified glovebox in the form of a light orange pyrophoric powder. A yield of 70 g (85%) of dilithioferrocene•tetramethylethylenediamine was then obtained.

\* To whom correspondence should be addressed. E-mail: ian.manners@bristol.ac.uk.

<sup>†</sup> University of Bristol.

<sup>‡</sup> University of Toronto.

<sup>§</sup> University of Massachusetts.

Table 1. Characterization of PFEMS and PS Homopolymers

| Table 1. Characterization of 1,2,3,4,5-pentakis(phenyl)-1,3,5-triazole and its corresponding polymers |         |       |             |       |                  |            |           |                             |              |      |
|---|---------|-------|-------------|-------|------------------|------------|-----------|-----------------------------|--------------|------|
|   | monomer |       | solvent     |       | initiator        |            | M/I ratio | $M_n$ (theory) <sup>a</sup> | $M_n$ (expt) | PDI  |
|   |         | (g)   |             | (mL)  |                  | ( $\mu$ L) |           | (g/mol)                     | (g/mol)      |      |
| 2a  | (1)     | 0.100 | THF         | 3.000 | <i>n</i> -BuLi   | 12.5       | 19.5:1    | 5000                        | 7800         | 1.04 |
| 2b  | (1)     | 0.100 | THF         | 3.000 | <i>n</i> -BuLi   | 4.2        | 58.5:1    | 15000                       | 19940        | 1.08 |
| 2c  | (1)     | 0.100 | THF         | 3.000 | <i>n</i> -BuLi   | 2.1        | 117.1:1   | 30000                       | 35660        | 1.06 |
| 4a  | styrene | 0.210 | cyclohexane | 1.000 | <i>sec</i> -BuLi | 8.0        | 180.0:1   | 18800                       | 28000        | 1.21 |

<sup>a</sup> Theoretical values of  $M_n$  (assuming a 100% conversion of monomer 1).

Table 2. Characterization of PS-*b*-PFEMS<sub>y</sub> Diblock Copolymers

|           | (1) (g) | THF (mL) | styrene (mL) | cyclohexane (mL) | <i>sec</i> -BuLi ( $\mu$ L) | living PS ( $\mu$ L) | isolated yield (%) | $M_n$ PS <sup>a</sup> (g/mol) | $M_n$ PS- <i>b</i> -PFEMS <sup>b</sup> (g/mol) | $x/y$ <sup>b</sup> | $\phi_{\text{PFEMS}}$ | PDI               |
|-----------|---------|----------|--------------|------------------|-----------------------------|----------------------|--------------------|-------------------------------|--|--------------------|-----------------------|-------------------|
| <b>3a</b> | 0.100   | 0.400    | 0.332        | 1.744            | 24.1                        | 210.1                | 84                 | 19800                         | 74000  | 188:211            | 0.69                  | 1.06              |
| <b>3b</b> | 0.105   | 0.400    | 0.200        | 1.000            | 25.0                        | 123.6                | 90                 | 10200                         | 51500  | 97:161             | 0.77                  | 1.07              |
| <b>3c</b> | 0.103   | 0.400    | 0.200        | 1.000            | 12.5                        | 122.4                | 97                 | 22430                         | 109500   | 213:340            | 0.76                  | 1.12              |
| <b>3d</b> | 0.178   | 0.400    | 0.200        | 1.000            | 8.0                         | 122.0                | 99                 | 27800                         | 253600   | 264:881            | 0.87                  | 1.17              |
| <b>3e</b> | 0.106   | 0.400    | 0.300        | 1.800            | 50.0                        | 213.0                | 42                 | 5400                          | 28110  | 51:89              | 0.77                  | 1.01 <sup>c</sup> |
| <b>3f</b> | 0.100   | 0.400    | 0.300        | 1.500            | 50.0                        | 184.0                | 44                 | 5100                          | 28600  | 48:92              | 0.79                  | 1.03 <sup>c</sup> |
| <b>3g</b> | 0.111   | 0.400    | 0.200        | 1.000            | 45.0                        | 126.0                | 63                 | 3640                          | 30600  | 35:105             | 0.86                  | 1.02 <sup>c</sup> |

<sup>a</sup> From the GPC of the aliquot. <sup>b</sup> From <sup>1</sup>H NMR integration. <sup>c</sup> After further purification by slow precipitation from THF into hexanes.

**Synthesis of Ethylmethylsila[1]ferrocenophane (1).** The monomer was prepared by adding distilled dichloroethylmethylsilane (7.9 mL, 58.7 mmol) to a  $-78$  °C suspension of dilithioferrocene-tetramethylethylenediamine (15.4 g, 49.0 mmol) in diethylether. The reaction was then allowed to slowly warm to room temperature over 12 h. The solvent was evaporated and replaced with hexanes for filtration through celite. The dark red crystals were further purified for anionic polymerization.<sup>31</sup> High yields (8.5 g were isolated, 69%) of this dark orange crystalline powder were stored under an inert atmosphere glovebox for future use in polymerizations. <sup>1</sup>H NMR ( $\text{C}_6\text{D}_6$ , 270 MHz):  $\delta$  0.36 (s, Si-CH<sub>3</sub>), 0.89 (q, Si-CH<sub>2</sub>CH<sub>3</sub>), 1.12 (t, Si-CH<sub>2</sub>CH<sub>3</sub>), 3.96 (m, *Cp*), 4.42 (m, *Cp*).

**Synthesis of the Homopolymer Poly(ferrocenylethylmethylsilane) (2), PFEMS.** The synthesis of the homopolymer was carried out to rule out any partial miscibility of the two blocks by a short DSC study. The living anionic ring-opening polymerization, which has been described in a previous paper,<sup>28</sup> yielded samples of controlled molecular weight and of low polydispersity (Yield  $\sim$  90%). <sup>1</sup>H NMR ( $\text{C}_6\text{D}_6$ , 270 MHz):  $\delta$  0.54 (s, Si-CH<sub>3</sub>), 1.03 (br, Si-CH<sub>2</sub>CH<sub>3</sub>), 1.12 (br, Si-CH<sub>2</sub>CH<sub>3</sub>), 4.04 (m, *Cp*), 4.21 (m, *Cp*). GPC data: see Table 1.

**Synthesis of the Diblock Copolymers Polystyrene-*block*-Poly(ferrocenylethylmethylsilane) (3), PS-*b*-PFEMS.** The synthesis of the diblock copolymers followed the method described previously.<sup>28</sup> However, for the ease of preparation of high PFS content diblock copolymers, a slight change in the protocol was made. In the case of higher PFEMS content block copolymers, to minimize error from the measurement of low volumes of styrene monomer and initiator, a larger batch of living polystyryl solution ( $\sim$ 10-fold excess) was prepared. Styrene monomer in cyclohexane was initiated with *sec*-BuLi (1.4 M) and left to polymerize for 30 min. One tenth of the solution was taken and added to a THF solution of 1 and the remainder was quenched for a molecular weight investigation by GPC. The living polymerization was left for an hour and was then quenched with dry, degassed methanol. Controlled, high molecular weights were achieved together with low polydispersity indices, as expected for living anionic polymerization, yielding air and moisture stable amorphous diblock copolymers. <sup>1</sup>H NMR ( $\text{CD}_2\text{Cl}_2$ , 400 MHz):  $\delta$  0.37 (s, Si-CH<sub>3</sub>), 0.86 (br, Si-CH<sub>2</sub>CH<sub>3</sub>), 0.97 (br, Si-CH<sub>2</sub>CH<sub>3</sub>), 1.43 (br, CH<sub>2</sub>CH-C<sub>6</sub>H<sub>5</sub>), 1.73 (br, CH<sub>2</sub>CH-C<sub>6</sub>H<sub>5</sub>), 3.94 (m, *Cp*), 4.14 (br, *Cp*), 6.51–7.00 (br, CH<sub>2</sub>CH-C<sub>6</sub>H<sub>5</sub>). The integration of the aromatic protons related to the polystyrene block and those of the cyclopentadienyl rings of the organometallic block permitted the calculation of the block ratio. The GPC analysis of the aliquot, that is, the polystyrene homopolymer 4a, obtained before adding the second monomer, gave the length of the first block and using the NMR integration the overall polymer molecular weight was estimated. GPC analysis of the dried diblock copolymer (yields  $\sim$ 90%, typical

amounts  $\sim$ 120 mg) indicated a monomodal molecular weight profile (Table 2).

**Calculation of *N* Using a Common Segment Volume.** Polymer segments of similar volume were added together to obtain *N*. The volume *V* of one mole of polymer is given by the ratio of its mass *M* and its density  $\rho$ . Therefore, the volume ratio between PS and PFS is  $V_{\text{PS}}/V_{\text{PFEMS}} = (M_{\text{PS}}/M_{\text{PFEMS}})(\rho_{\text{PFEMS}}/\rho_{\text{PS}})$  and is equal to 0.50. The total number *N* of repeat unit of a similar volume in a PS-*b*-PFEMS diblock copolymer is then calculated adding the repeat units of PFEMS and half the repeat units of PS. For instance, 3a has a *N* of 211 + 188/2 = 305.

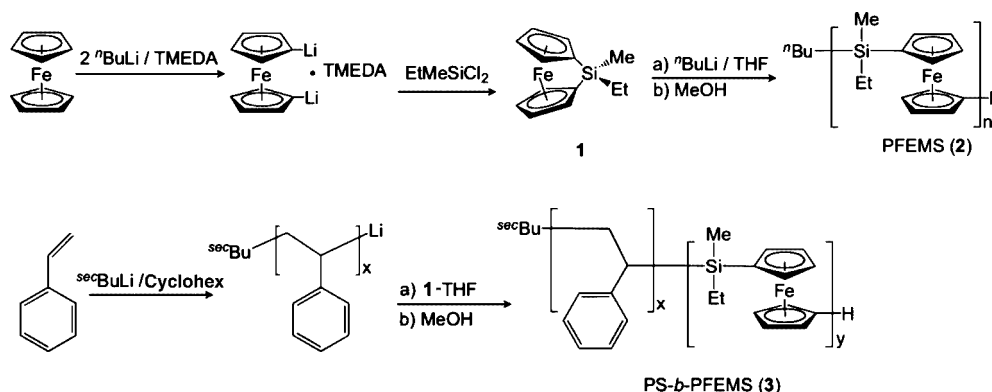
## Results and Discussion

To obtain controllable molecular weights and narrow polydispersities, all polymerizations involved a living anionic route (Scheme 1).<sup>32,33</sup> Investigations such as gel permeation chromatography (GPC), <sup>1</sup>H NMR, and plots of molecular weights versus the ratio between the monomer and its initiator were used to confirm the narrow polydispersity, the overall molecular weight of the diblock and the volume fraction of the two blocks and to testify to the living character of the polymerization, respectively.

**Syntheses of Ferrocenophane Monomer (1), Homopolymer (2), and Diblock Copolymer (3).** The synthesis of the ring-strained ferrocenophane monomer, ethylmethylsila[1]-ferrocenophane (1), has been reported in a previous paper.<sup>32</sup>

Syntheses of poly(ferrocenylethylmethylsilane) homopolymers (2) were carried out following the same procedure as published elsewhere.<sup>28</sup> A summary of the synthetic experiments is presented in Table 1. The living character of the polymerization was confirmed by the linearity of the plot of various homopolymer molecular weights versus the monomer-to-initiator ratio (Figure 1). Monomodal, narrow molecular weight distributions were observed in the GPC traces (Figure 2a,d) for the organic block alone and the diblock, respectively. When necessary, that is, when a second, higher molecular weight peak appeared in the GPC traces (Figure 2b,c), a drop by drop precipitation into hexanes from a tetrahydrofuran solution was conducted to separate longer polymer chains obtained by polymer coupling upon quenching (see note (c) in Table 2). The remaining solution was precipitated again to reach a narrow polydispersity and monomodal GPC trace (Figure 2d). In the case of a diblock synthesis, where the first block can still be

**Scheme 1. Syntheses of Poly(ferrocenylethylmethylsilane) (PFEMS) and Polystyrene-*block*-poly(ferrocenylethylmethylsilane) (PS-*b*-PFEMS) from a [1]Ferrocenophane Monomer**



present (Figure 2b), the same technique was also applied for purification.

The syntheses of polystyrene-*block*-poly(ferrocenylethylmethylsilane) (**3**) with different volume fractions of the organometallic block were performed using sequential living anionic polymerization of styrene and ferrocenophane **1**, analogous to the procedure described previously<sup>28</sup> and summarized in Table 2.

Diblock molecular weights were calculated using the molecular weight of the corresponding polystyrene and the ratio

calculated from the integration of the peaks from <sup>1</sup>H NMR. As the polystyrene block was shorter, the comparative integration was carried out using the aromatic protons of the phenyl group versus the cyclopentadienyl protons from the ferrocene unit. The integration gave a ratio between the two blocks, which was then combined to their respective homopolymer densities ( $\rho_{\text{PFEMS}} = 1.29 \text{ g/cm}^3$ ,  $\rho_{\text{PS}} = 1.05 \text{ g/cm}^3$ )<sup>15</sup> to obtain volume fractions.

**Preparation of Bulk Samples.** The diblock copolymers were cast from toluene and annealed to achieve self-assembly. The preparation of the bulk samples was conducted using a previously reported technique<sup>28</sup> that allows a concentrated solution to form a thick film on a glass slide. Annealing in a solvent chamber<sup>34</sup> at room temperature was used as a preannealing step, allowing the polymer chains to order over a short period of time, reducing the time of subsequent thermal annealing. The latter was conducted in a vacuum oven at around 150 °C over 5 days. Considerable care was taken in cooling the samples down before exposing them to air as oxidation of the polymer in air has been observed at elevated temperature.

**Thermal Characterization of PS-*b*-PFEMS Diblock Copolymers.** Diblock copolymers with a low volume fraction of PFEMS have been shown to be amorphous in our previous studies.<sup>28</sup> For the diblock copolymers with a higher volume fraction of PFEMS, no melting point or crystallization temperature was observed on DSC scans from −50 to 300 °C, indicating that these diblock copolymers are also amorphous. Furthermore, DSC cycles over this temperature range have been performed on four of the high PFEMS content diblock copolymers as well as on PS and PFEMS homopolymers. Shown in Figure 3 are scans of PFEMS (**2c**) and PS (**4a**) homopolymers and a diblock copolymer of PFEMS volume fraction of 0.69 (**3a**). The diblock copolymer exhibited two glass transition temperatures (31 and 92 °C). The first one was associated with the metal-containing PFEMS block and the second related to the organic block. The glass transition temperatures obtained were consistent with those of the corresponding homopolymers. The presence of two distinct glass transition temperatures indicated no or very poor partial miscibility and hence, microphase separation.

**Morphology Characterization of PS-*b*-PFEMS Diblock Copolymers.** The morphologies of a series of PS-*b*-PFEMS diblock copolymers were studied by TEM and SAXS and the results were gathered in a morphology diagram. Figure 4A, C, and E, samples **3a**, **3c** and **3d**, respectively, showed the three stable morphologies, lamellae, cylinders, and spheres, respec-

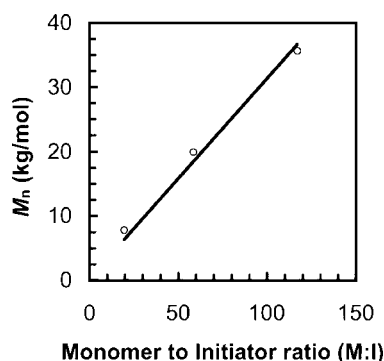


**Figure 1.** Plot of the molecular weights of **2a**, **2b**, and **2c** versus monomer-to-initiator ratio.

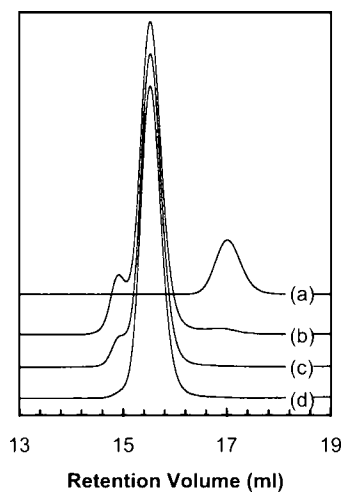


**Figure 2.** GPC traces, in THF at 25 °C, of (a) polystyrene aliquot ( $M_n = 5400$ ), (b) PS-*b*-PFEMS (**3e**) after synthesis with presence of PS homopolymer and coupled chains, (c) PS-*b*-PFEMS after removal of the PS aliquot traces, and (d) the same diblock copolymer after removal, by precipitation, of larger, coupled chains.



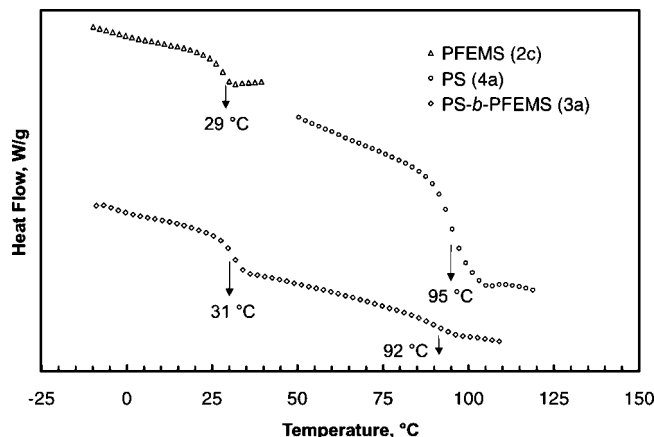


Figure 3. DSC scans of 2c, 4a, and 3a. Scan rate: 10 K/min.

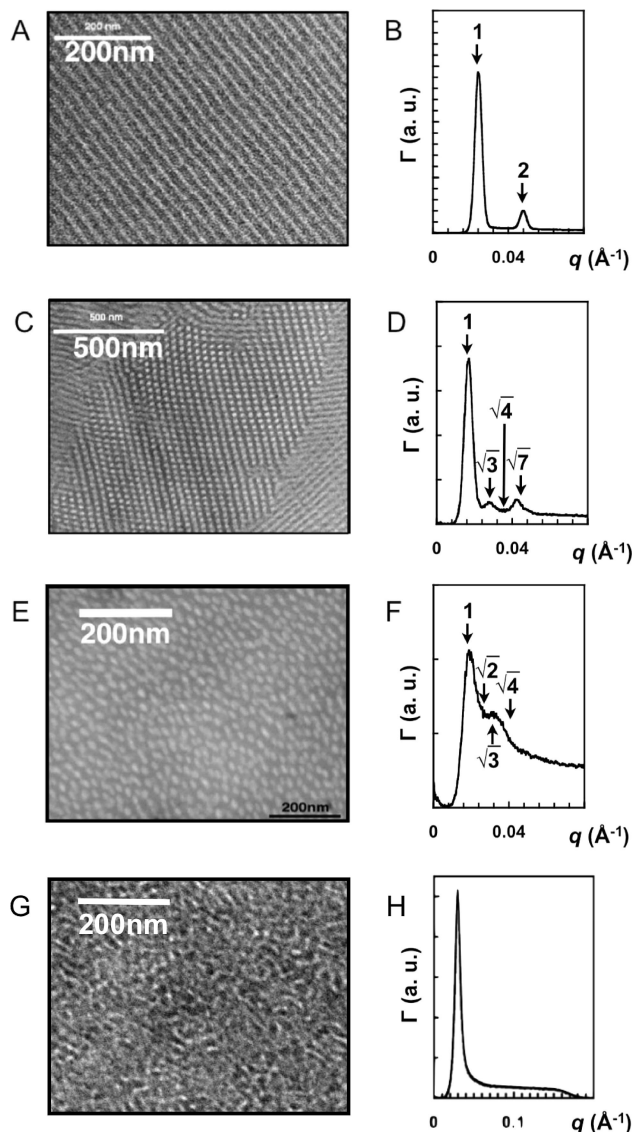


Figure 4. Bright field TEM images (A, C, E, and G) and SAXS patterns (B, D, F, and H) for PS-*b*-PFEMS samples 3a, 3c, 3d, and 3b, respectively.

tively. A disordered morphology has also been observed under TEM (Figure 4G), and the lack of specific order has been confirmed by SAXS (Figure 4H).

In Figure 4A, C, E, and G, the excellent contrast observed on TEM images was obtained by microtoming thin layers of a

bulk sample, the high electron density of the iron-containing PFEMS block provides sufficient contrast for TEM imaging without the necessity of staining. The images were recorded in the bright field mode, thus the organic blocks were bright in comparison with the more electron dense polyferrocenylsilane blocks.

Morphologies ranging from spheres to hexagonal packed cylinders to lamellae have already been studied<sup>28</sup> from polystyrene-*block*-poly(ferrocenylethylmethylsilane) with low PFEMS contents ( $\phi_{\text{PFEMS}} = 0.07$  to  $\phi_{\text{PFEMS}} = 0.68$ ). With a slight increase of the volume fraction to  $\phi_{\text{PFEMS}} = 0.69$ , the diblock copolymer adopted an asymmetric lamellae morphology. Shown in Figure 4A is the TEM image where the PFEMS lamellae were thicker (about double the width) than the organic corresponding domains. The formation of a lamellar morphology was further confirmed by SAXS (see Figure 4B) and was evidenced by a ratio of Bragg reflections of 1:2. The lamellar microdomain spacing  $d$  was estimated to be 26 nm, and the thicknesses of PFEMS and PS domains were 18 and 8 nm, respectively.<sup>35</sup>

A close-packed hexagonal cylindrical morphology was also investigated by use of a sample with  $\phi_{\text{PFEMS}} = 0.76$ . The TEM bright field image in Figure 4C presented well-ordered hexagonally packed PS cylinders distributed in the PFEMS matrix. The SAXS profiles (Figure 4D) showed Bragg reflections with a ratio of  $1:\sqrt{3}:\sqrt{4}:\sqrt{7}$ , where the  $\sqrt{4}$  reflection was absent due to form factor cancellation.<sup>36</sup> The cylinder–cylinder distance ( $D_{\text{cyl-cyl}}$ ) was calculated to be 42 nm from eq 1, with  $q^*$  being the first peak, and the diameter of the cylinders was 18 nm using eq 2, derived from the volume ratio of four cylinders packed in a hexagonal lattice.

$$D_{\text{cyl-cyl}} = \frac{2\pi}{q^*} \sqrt{\frac{4}{3}} \quad (1)$$

$$d_{\text{cyl}} = \sqrt{\frac{\phi_{\text{PFEMS}} D_{\text{cyl-cyl}}^2}{\pi \sqrt{2}}} \quad (2)$$

$$D_{\text{s-s}} = \frac{2\pi}{q^*} \sqrt{\frac{3}{2}} \quad (3)$$

The body centered cubic (BCC) spherical morphology as well as the disordered spherical morphology appeared in a narrow volume fraction region for high PFEMS contents ( $\phi_{\text{PFEMS}} = 0.87$ ). Long-range order could be achieved by adding a homopolymer to the diblock to relieve the frustrated chains from their low order configuration, as described previously.<sup>23</sup> The SAXS profile of asymmetric diblock copolymer 3d with  $\phi_{\text{PFEMS}} = 0.87$  in Figure 4F showed a ratio of Bragg reflections at  $1:\sqrt{3}$ , indicating either a cylindrical or a spherical morphology. The corresponding bright field TEM image (Figure 4E) showed a PFEMS matrix surrounding PS spherical nanodomains. The presence of spheres instead of cylinders was further indicated by the analysis of the TEM images from slices taken at different angles, which showed a spherical symmetry of the PS domains. The polystyrene domains were separated by a distance of 41 nm according to the SAXS profile (Figure 4F) and eq 3.

Disordered morphologies were also observed for systems of lower molecular weight for PFEMS volume fractions between 0.77 and 0.86. When sample 3b was cast and annealed, as described earlier, it did not show any sign of particular regular order, although two phases could be identified. In the TEM image (Figure 4G), phase separation was observed and a lack of ordering was validated by the SAXS pattern in Figure 4H. The first peak  $q^*$  indicated phase separation and a domain size of approximately 21 nm based on a lamellar structure and 25 nm using the cylindrical assumption in eq 1.

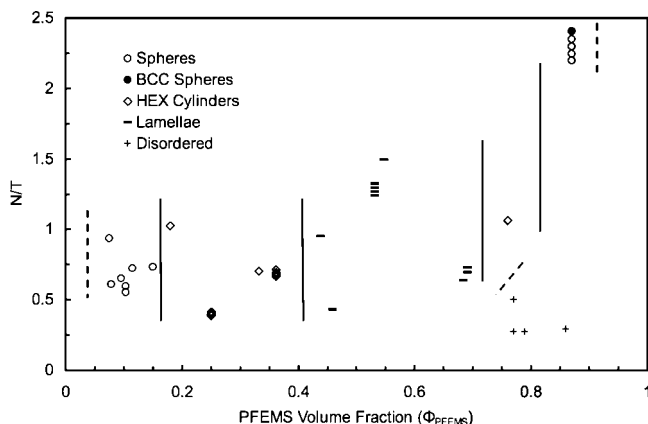


**Figure 5.** Diagram of the equilibrium morphologies of the solid state self-assembly of PS-*b*-PFEMS. Straight lines represent approximate order–order transitions and dotted lines represent the order–disorder transitions.

**Morphology Diagram for PS-*b*-PFEMS Diblock Copolymers.** Diblock copolymer morphology diagrams, as described and studied by, for example, Leibler,<sup>37</sup> Bates,<sup>38</sup> Hashimoto,<sup>39</sup> and Kawasaki,<sup>40</sup> as well as by Thomas and Vancso<sup>23</sup> and Rehahn<sup>41</sup> (for PFS-based diblock systems), illustrate the order–order and order–disorder transitions (OOT and ODT, respectively) with respect to the volume fraction of one of the components and the product of the Flory–Huggins parameter  $\chi$  with the number  $N$  of Kuhn steps. In the two last examples, the focus was on potentially crystallizable poly(ferrocenyldimethylsilane), PFDMS, presenting either a complete morphology diagram built from neat diblocks and blended systems<sup>23</sup> or studying the low PFDMS contents in PFDMS-*b*-PMMA diblock copolymers. In Figure 5, a morphology diagram of the amorphous system PS-*b*-PFEMS is presented. The diagram consists of previously reported information<sup>28</sup> and data from Table 2. The volume fraction of the organometallic block is plotted against  $N/T$ , which is proportional to  $\chi N^{2/3}$  over a wide range of diblock copolymer ratios.  $N$  here is calculated based on a common segment volume, polystyrene repeat units being 50% of the PFEMS units volume. The solid lines represented on the diagram are not well-defined OOTs nor are the dotted lines ODTs.<sup>42</sup> Their purpose is to guide the eye to areas of consistent morphology. As expected by the anticipated difference in Kuhn lengths of the two blocks, the morphology diagram is asymmetric in terms of volume fraction, with smaller areas for consistent morphologies for higher PFEMS content, with the lamellae morphology area being off-centered from  $\phi_{\text{PFEMS}} = 0.50$ . The diagram shows also an asymmetry regarding the order–disorder limit, where the ODT at low  $\chi N$  is shifted at higher molecular weights (50 kg/mol) for  $\phi_{\text{PFEMS}} = 0.77$  compared to a 39 kg/mol diblock copolymer that shows cylindrical morphology for  $\phi_{\text{PFEMS}} = 0.25$ .

## Summary

The living anionic polymerization of sila[1]ferrocenophane monomers described previously by our group<sup>9,28</sup> has proven to be useful for the synthesis of high PFEMS content block copolymers. Living polystyryl chains initiated sila[1]ferrocenophane monomer (**1**) to generate high  $DP_n$  organometallic blocks with narrow and monomodal molecular weight distributions. The new diblock copolymers readily self-assemble in the bulk to give expected morphologies. These morphologies, with the organometallic block being the continuous matrix, may have a variety of potential applications, for example, as templates for one-

step nanolithography where highly ordered pits may be formed in a substrate.

**Acknowledgment.** I.M. acknowledges support for a Marie Curie Chair from the European Union and a Royal Society Wolfson Research Merit Award at Bristol. T.P.R. acknowledges funding from the U.S. Department of Energy, DEF0296ER45612.

## References and Notes

- (1) Bates, F. S. *Science* **1991**, *251*, 898–905.
- (2) Alexandridis, P.; Lindman, B., *Amphiphilic Block Copolymers*. Elsevier Science B. V.: Amsterdam, 2000; p 435.
- (3) Krausch, G.; Magerle, R. *Adv. Mater.* **2002**, *14*, 1579–1583.
- (4) Park, C.; Yoon, J.; Thomas, E. L. *Polymer* **2003**, *44*, 6725–6760.
- (5) Eloi, J.-C.; Chabanne, L.; Whittell, G. R.; Manners, I. *Mater. Today* **2008**, *11*, 28–36.
- (6) Higashihara, T.; Faust, R. *Macromolecules* **2007**, *40*, 7453–7463.
- (7) Whittell, G. R.; Manners, I. *Adv. Mater.* **2007**, *19*, 3439–3468.
- (8) Bellas, V.; Rehahn, M. *Angew. Chem., Int. Ed.* **2007**, *46*, 5082–5104.
- (9) Ni, Y. Z.; Rulkens, R.; Manners, I. *J. Am. Chem. Soc.* **1996**, *118*, 4102–4114.
- (10) Eitouni, H. B.; Balsara, N. P. *J. Am. Chem. Soc.* **2004**, *126*, 7446–7447.
- (11) Rider, D. A.; Winnik, M. A.; Manners, I. *Chem. Commun.* **2007**, 4483–4485.
- (12) Li, J. K.; Zou, S.; Rider, D. A.; Manners, I.; Walker, G. C. *Adv. Mater.* **2008**, *20*, 1989–1993.
- (13) Korczagin, I.; Lammertink, R. G. H.; Hempenius, M. A.; Golze, S.; Vancso, G. J. Surface Nano- and Microstructuring with Organometallic Polymers. In *Ordered Polymeric Nanostructures at Surfaces*; Vancso, G. J., Reiter, G., Eds.; Springer Berlin: Heidelberg, 2006; Vol. 200, pp 91–117.
- (14) Lu, J.; Chamberlin, D.; Rider, D. A.; Liu, M. Z.; Manners, I.; Russell, T. P. *Nanotechnology* **2006**, *17*, 5792–5797.
- (15) Paquet, C.; Cyr, P. W.; Kumacheva, E.; Manners, I. *Chem. Mater.* **2004**, *16*, 5205–5211.
- (16) Rider, D. A.; Liu, K.; Eloi, J.-C.; Vanderark, L.; Yang, L.; Wang, J.-Y.; Grozea, D.; Lu, Z.-H.; Russell, T. P.; Manners, I. *ACS Nano* **2008**, *2*, 263–270.
- (17) Hinderling, C.; Keles, Y.; Stoeckli, T.; Knapp, H. F.; De Los Arcos, T.; Oelhafen, P.; Korczagin, I.; Hempenius, M. A.; Vancso, G. J.; Pugin, R.; Heinzelmann, H. *Adv. Mater.* **2004**, *16*, 876–879.
- (18) Lastella, S.; Jung, Y. J.; Yang, H.; Vajtai, R.; Ajayan, P. M.; Ryu, C. Y.; Rider, D. A.; Manners, I. *J. Mater. Chem.* **2004**, *14*, 1791–1794.
- (19) Lu, J. Q.; Kopley, T. E.; Moll, N.; Roitman, D.; Chamberlin, D.; Fu, Q.; Liu, J.; Russell, T. P.; Rider, D. A.; Manners, I.; Winnik, M. A. *Chem. Mater.* **2005**, *17*, 2227–2231.
- (20) Datta, U.; Rehahn, M. *Macromol. Rapid Commun.* **2004**, *25*, 1615–1622.
- (21) Eitouni, H. B.; Balsara, N. P.; Hahn, H.; Pople, J. A.; Hempenius, M. A. *Macromolecules* **2002**, *35*, 7765–7772.
- (22) Kloninger, C.; Knecht, D.; Rehahn, M. *Macromolecules* **2004**, *37*, 8319–8324.
- (23) Lammertink, R. G. H.; Hempenius, M. A.; Thomas, E. L.; Vancso, G. J. *J. Polym. Sci., Part B: Polym. Phys.* **1999**, *37*, 1009–1021.
- (24) Lammertink, R. G. H.; Hempenius, M. A.; Vancso, G. J. *Langmuir* **2000**, *16*, 6245–6252.
- (25) Lammertink, R. G. H.; Hempenius, M. A.; Vancso, G. J.; Shin, K.; Rafailovich, M. H.; Sokolov, J. *Macromolecules* **2001**, *34*, 942–950.
- (26) Li, W.; Sheller, N.; Forster, M. D.; Balaishis, D.; Manners, I.; Annis, B.; Lin, J. S. *Polymer* **2000**, *41*, 719–724.
- (27) Massey, J. A.; Power, K. N.; Winnik, M. A.; Manners, I. *Adv. Mater.* **1998**, *10*, 1559–1562.
- (28) Rider, D. A.; Cavicchi, K. A.; Power-Billard, K. N.; Russell, T. P.; Manners, I. *Macromolecules* **2005**, *38*, 6931–6938.
- (29) Rider, D. A.; Cavicchi, K. A.; Vanderark, L.; Russell, T. P.; Manners, I. *Macromolecules* **2007**, *40*, 3790–3796.
- (30) Bishop, J. J.; Davison, A.; Katcher, M. L.; Lichtenberg, D. W.; Merrill, R. E.; Smart, J. C. *J. Organomet. Chem.* **1971**, *27*, 241–249.
- (31) For further information on the synthesis and purification of the monomer, see ref 28.
- (32) Flory, P. J. *Principles of Polymer Chemistry*; Cornell University Press: Ithaca, NY, 1953; Vol. xvi, p 672.
- (33) Szwarc, M. *Makromol. Chem. Rapid Commun.* **1992**, *13*, 141–145.
- (34) Although applied mainly to thin films, this technique has been successful in terms of bulk annealing if followed by a milder (few degrees lower) thermal annealing. For information about the solvent annealing techniques, see: (a) Cavicchi, K. A.; Russell, T. P. *Macromolecules* **2007**, *40*, 1181–1186. (b) Kim, S. H.; Misner, M. J.; Xu, T.; Kimura, M.; Russell, T. P. *Adv. Mater.* **2004**, *16*, 226–231.

- (35) We quote domain sizes from SAXS because of the potential shear-induced distortion of the domains in TEM images. The sizes are nevertheless similar in both techniques (from TEM images, results given for the periodicity of the PS domains: for the lamellar system, 25 nm; for the hexagonal system, 38 nm; and for the spherical system, 34 nm).
- (36) Pedersen, J. S. *Adv. Colloid Interface Sci.* **1997**, 70, 171–210.
- (37) Leibler, L. *Macromolecules* **1980**, 13, 1602–1617.
- (38) Matsen, M. W.; Bates, F. S. *Macromolecules* **1996**, 29, 1091–1098.
- (39) Hasegawa, H.; Tanaka, H.; Yamasaki, K.; Hashimoto, T. *Macromolecules* **1987**, 20, 1651–1662.
- (40) Ohta, T.; Kawasaki, K. *Macromolecules* **1986**, 19, 2621–2632.
- (41) Kloninger, C.; Rehahn, M. *Macromolecules* **2004**, 37, 8319–8332.
- (42) Khandpur, A. K.; Foerster, S.; Bates, F. S.; Hamley, I. W.; Ryan, A. J.; Bras, W.; Almdal, K.; Mortensen, K. *Macromolecules* **1995**, 28, 8796–8806.

MA8012493